

3D simulation of micromegas detector performance^{*}

GUO Jun-Jun(郭军军)¹⁾ WANG Xiao-Lian(汪晓莲)²⁾ TANG Hao-Hui(唐浩辉)
ZHAO Yan-E(赵艳娥) XU Zi-Zong(许咨宗)

University of Science and Technology of China, Hefei 230026, China

Abstract Micromegas (MICRO MESH Gaseous Structure) is a position-sensitive gaseous detector. It is widely used in particle physics. We present the results of full 3D Monte Carlo simulations of Micromegas performance, taking into account all the processes from the primary ionization, the electron collection efficiency, and the gain to the signal formation. The simulation results are in good agreement with experimental data.

Key words Micromegas, simulation, primary ionization, gain, signal

PACS 29.40.Cs, 29.85.-c

1 Introduction

The MICRO MESH Gaseous Structure (Micromegas), which was invented in 1995 at Saclay of France, is a kind of gaseous detector based on a simple geometry with planar electrodes [1]. The detector is reliable, cheap and able to accommodate high-particle flux. It consists of a drift gap and a 50–100 μm amplification gap separated by a thin mesh. The primary ionization happens in the drift gap. The primary electrons follow the electric field lines into the amplification gap where they are multiplied by avalanche due to the high field. The printed electrodes collect the electrons from the avalanche.

Micromegas is a suitable candidate in high-intensity X-ray detection and tomography. With its simple structure and low cost, it has been adopted by many experiments in particle physics experiments, such as TPC for ILC, tracking in nuclear physics experiment COMPASS, axion CAST, hadronic calorimetry DHCAL, and neutrino NOSTOS.

In order to study the properties of Micromegas, a full 3D simulation has been performed: from the model building and primary ionization to the signal formation. And we use some specific software packages, such as Maxwell which calculates three dimensional electric fields [2] and Garfield [3]. The results of simulation are compared with the experimental data.

2 Micromegas structure

A detailed description of the Micromegas is given in Ref. [4]. In our experiment the drift electrode is made from 5 cm \times 5 cm 500 lines per inch (LPI) steel mesh and the same mesh is used as the amplification electrode. The diameter of steel wire is near 20 μm . The thickness of conversion gap is 3 mm. Nylon fish fibers of 100 μm with 2 mm pitch, which keeps the 100 μm thickness of amplification gap, are stretched and glued on one side of PCB. The signal induced on the anode is amplified and shaped by ORTEC 142AH preamplifier [5] and observed on an oscilloscope or measured by a multi-channels analyzer (MCA). The Micromegas is operated in the gas mixture of 90%argon+10%isobutane, at a temperature of 300 K and a pressure of 1 atm. The properties of the gas mixture are calculated by Magboltz [6].

3 Performance of micromegas detector

3.1 Primary ionization of 5.9 keV photon

The distribution of the number of primary electron-ion pairs produced in the 3 mm drift gap by 5.9 keV photons is shown in Fig. 1(a). Heed is a program that computes in detail the energy loss of

Received 13 May 2009

^{*} Supported by National Natural Science Foundation of China (10775132)

1) E-mail: xtguojj@mail.ustc.edu.cn

2) Corresponding author, E-mail: wangxl@ustc.edu.cn

©2009 Chinese Physical Society and the Institute of High Energy Physics of the Chinese Academy of Sciences and the Institute of Modern Physics of the Chinese Academy of Sciences and IOP Publishing Ltd

fast charged particles in gases, and it can simulate the absorption of photons through photo-ionization in gaseous detectors [7]. The peak in Fig. 1(a) corresponds to the escape peak (108± pairs of primary electron-ions) and a total energy peak (229± pairs of primary electron-ions) in the argon. Fig. 1(b) shows the spectra measured from the module which is the same as the one in simulation. The ratio of the 5.9 keV total energy peak and escape peak position

in the simulation is 2.1, which is nearly consistent with the experimental value 1.9. And in the experiment the energy resolution for the 5.9 keV peak is 27%, which is worse than the simulation, and it can be explained by the number fluctuation of the electrons which entered into the mesh and the electron gain in the amplification gap in the experiment. The ratio of count numbers between the escape peak and 5.9 keV peak depends on the detector geometry.

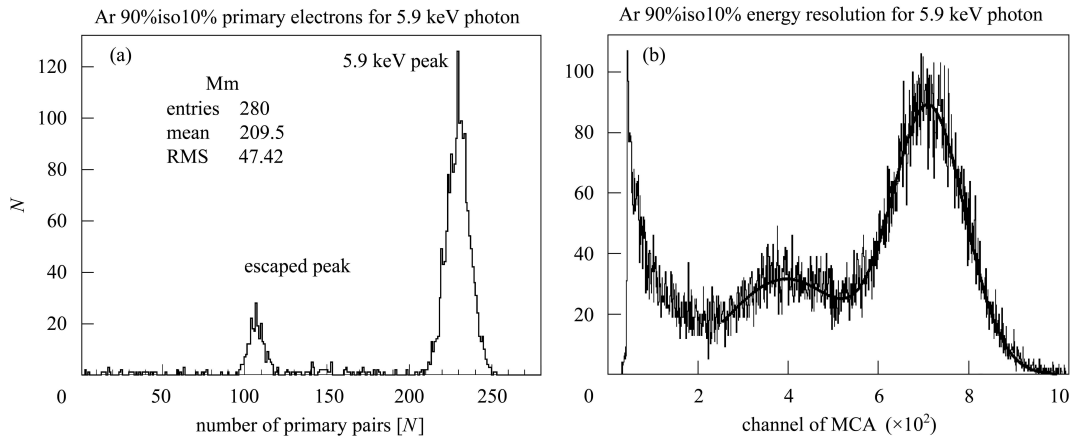


Fig. 1. (a) The number of primary electrons of and ^{55}Fe photon source in 3 mm drift gap in the argon90%+isobutane10% gas mixture; (b) The experimental energy spectrum of 5.9 keV photon measured by MCA. The energy resolution is 27%.

3.2 Electron collection efficiency

To calculate the electric field map in a given voltage supplied to Micromegas, a 3D-model is built by Maxwell. An elementary “unit” with dimensions of $500\ \mu\text{m} \times 50\ \mu\text{m} \times 150\ \mu\text{m}$, is built into the Maxwell model for the simulation. We choose the Micromegas chamber model with a drift gap of 3 mm, and an amplification gap of $100\ \mu\text{m}$. The mesh density is 500LPI with a thickness of $20\ \mu\text{m}$ and the size of the squared hole is $30\ \mu\text{m} \times 30\ \mu\text{m}$. The dimension of the copper anode unit is $500\ \mu\text{m} \times 50\ \mu\text{m} \times 10\ \mu\text{m}$. In Maxwell, the electric field map is calculated by a finite elements method, and the error on the field energy is less than 0.02%. In the field map, the bound field is set tangential to the lateral faces. The simulation of an entire Micromegas is done by periodically repeating this elementary “unit”.

Figure 2(a) shows the drift lines of electrons and ions released at the cathode and anode respectively. The electron lines are compressed towards the center of the hole and exhibit a funnel-like shape with a diameter of a few microns in the amplification region. This particular shape of the field insures a good col-

lection efficiency of the electron from the drift to the amplification gap. In the amplification gap, most of the ions are collected on the mesh in 50–100 ns and only few of them escape to the drift gap [8].

Some primary electrons may not drift into the amplification gap, since some drift lines of electrons above the mesh do not enter into the holes and end up on the mesh surface, as shown in Fig. 2(b). The ratio of the number of electrons entering the amplification gap over the number of primary electrons is defined as “electron collection efficiency”. With high electron collection efficiency we can get better energy resolution and a more precise track fit. The electron collection efficiency represents a very important parameter to be studied. The diffusion effect near the mesh also affects the collection efficiency.

Garfield is used to study the collection efficiency as a function of electric fields. Primary electrons are generated at a random position in the area of 140–240 μm above the mesh and the microscopic method is used: the electron track is recorded at the molecular level using Monte Carlo techniques, and this method relies heavily on the Magboltz procedures and gives results which are statistically compatible with

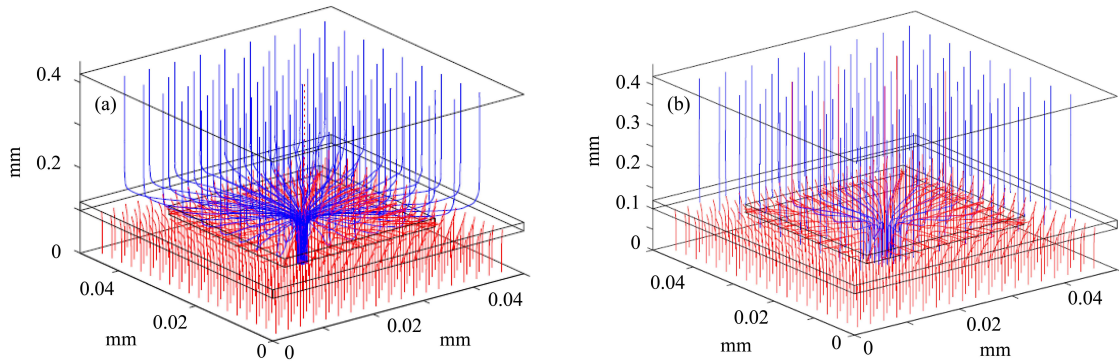


Fig. 2. (a) Electric field configuration at $E_{\text{amp}}/E_{\text{drift}}=420$; (b) Electric field configuration at $E_{\text{amp}}/E_{\text{drift}}=21$.

Magboltz tables [3]. For a given thickness and hole size and pitch, the collection efficiency increases as $E_{\text{amp}}/E_{\text{drift}}$ increases, and saturates when $E_{\text{amp}}/E_{\text{drift}}$ reaches a certain value. The collection efficiency is sensitive to the hole size and the thickness of the mesh. In our experiment, the thickness of the mesh is 20 μm and the size of the hole is 30 $\mu\text{m} \times 30 \mu\text{m}$. We change the voltage of the drift electrode keeping the grid voltage constant (i.e. avalanche gain is fixed) and measure the spectra of 5.9 keV X-rays. The peak of spectra is a measure of the number of the primary electrons collected by the amplification gap. The normalized peaks are equivalently the relative collection efficiencies for comparison with the simulation results. As shown in Fig. 3, the results of experiments and simulations with the same parameters of 500LPI mesh are roughly consistent. In the region $E_{\text{amp}}/E_{\text{drift}} > 400$, the collection efficiency is approximately constant.

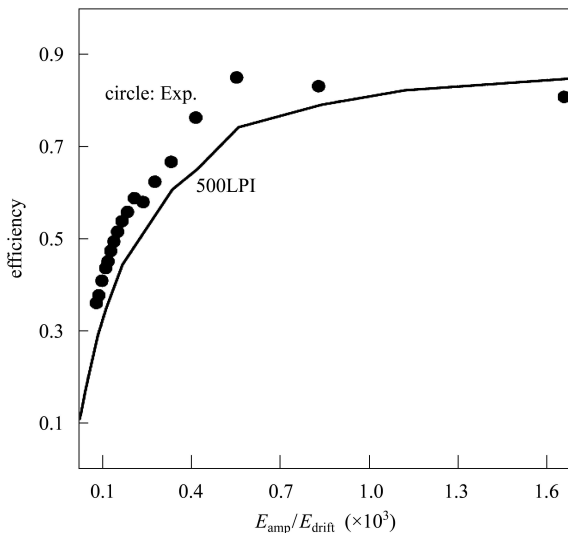


Fig. 3. Electron collection efficiency comparison of simulation with experiment (circle).

3.3 The gain

Garfield is used to study the gain of Micromegas. Because the size of the amplification gap is much smaller than the drift gap, only the primary ionizations occurring in the drift gap are considered. In the simulation, electrons are released in the center of a hole and avalanche happens in the amplification gap. The complete avalanche development is simulated by Garfield, and the simulation performs microscopic tracking of an electron and its secondary, using microscopic method [3].

The electron multiplication (M) is described by

$$M = \frac{Q}{Q_0} = \frac{N}{N_0}. \quad (1)$$

The spectra of 5.9 keV X-rays are measured and the data acquisition time is 300 s for every measurement. The electronics system calibration formula is

$$A = -8.76223 + 2.4475Q, \quad (2)$$

where A is the 5.9 keV total energy peak location, and Q is the input electric charge. The number of primary electron-ion pairs (N_0) produced in the 3 mm drift gap can be calculated by

$$N_0 = E/\varepsilon_0, \quad (3)$$

where E is the X-ray energy deposited in the gas, and ε_0 is the average energy to create one primary electron-ion pair, the formula is

$$\varepsilon_{0ij}^{-1} = \varepsilon_{0i}^{-1} \cdot \frac{Z'_i P_i}{Z'_i P_i + Z'_j P_j} + \varepsilon_{0j}^{-1} \cdot \frac{Z'_j P_j}{Z'_i P_i + Z'_j P_j}, \quad (4)$$

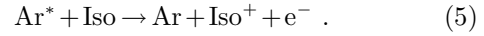
where ε_{0i} , P_i , Z'_i and ε_{0j} , P_j , Z'_j are the average energy to create one primary electron-ion pair, the pressure proportion and the effective atomic number in the i and j gas, respectively, and ε_0 is calculated with the data of argon and isobutane.

Figure 4(a) gives the gain with different voltages in different argon-isobutane gas mixtures. It shows

that the gain decreases with the increase of the percentage of isobutane, as the average energy of the avalanche electrons decreases with more isobutane. However, larger gain may lead to larger discharge probability. We choose appropriate gas mixture to make sure that Micromegas works normally.

The experimental data are larger than the simulation results because the penning effect in the gas mixture is not taken into account by Magboltz [9]. In the gas mixture, the excited molecules of argon sometimes transfer their excess energy to isobutane. As the ionization level of isobutane, which is 10.7 eV, is lower than the excitation levels of argon, which are

11.55 eV, 13.0 eV, and 14.0 eV for S, P, and D excitation level, respectively, then additional ionization will happen. This mechanism is known as penning effect and it can greatly enhance the multiplication. The process is:



The penning effect is added in simulation, and the percent of argon ions which participate in the penning effect is 26%, 33%, 35%, 50% in Ar95%, Ar90%, Ar85%, Ar80% gas mixtures, respectively. The simulation results shown in Fig. 4(b) are consistent with experiment.

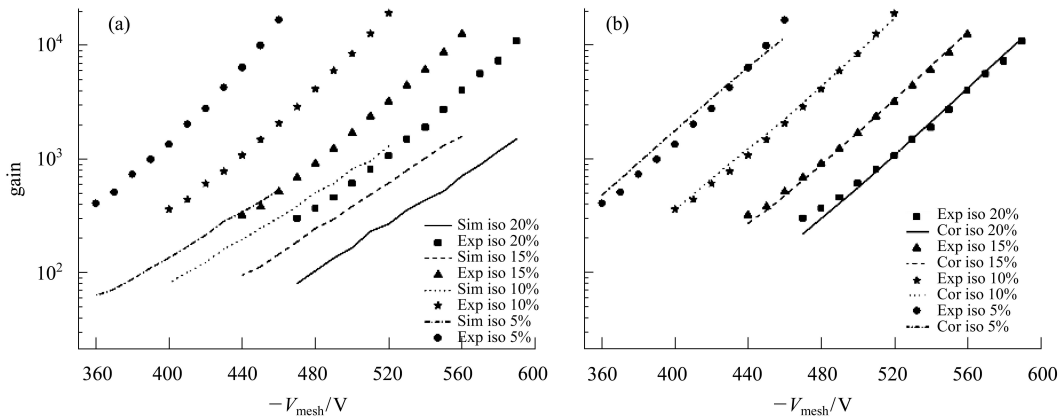


Fig. 4. (a) Gain vs. mesh voltage in different proportion of argon and Isobutane with the comparison of the experiment (Exp) and simulation (Sim), and the amplification gap is 120 μm ; (b) Gain vs. mesh voltage with the comparison of the experiment (Exp) and simulation with the penning effect added (Cor).

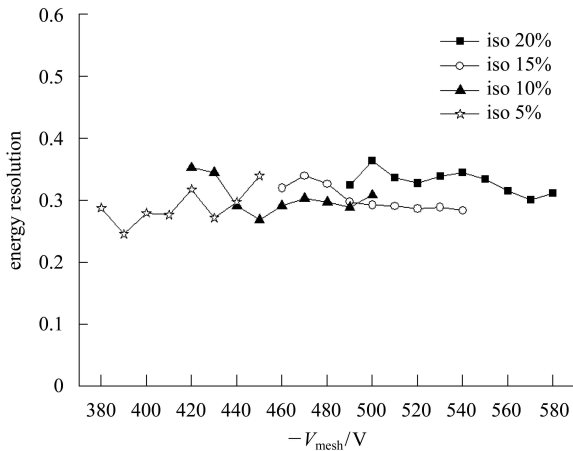


Fig. 5. The energy resolution vs the mesh voltage in different gas mixtures.

Figure 5 shows the energy resolution at different voltages in different argon-isobutane gas mixtures in the experiment, the resolutions change around 30%, and do not change with different voltages of mesh in different gas mixtures.

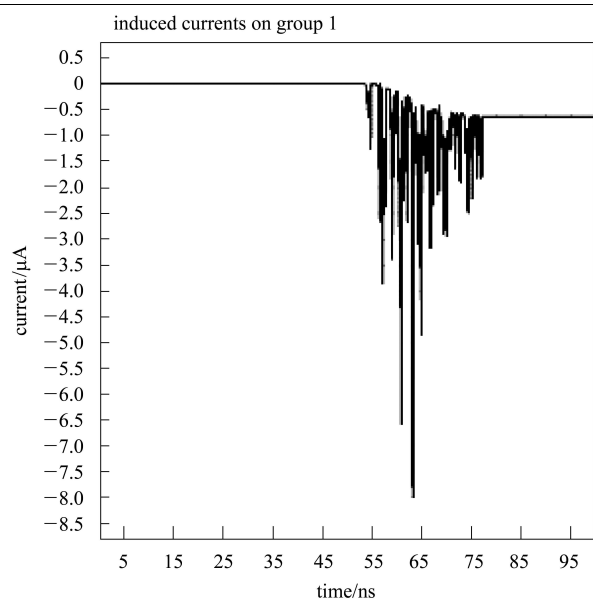


Fig. 6. Induced current on the anode, with $V_{\text{mesh}} = -490$ V and $V_{\text{drift}} = -510$ V.

3.4 Signal

The current induced between an electrode and ground due to a moving charge q can be calculated using the Ramo's theorem [10]. The signal is induced on the readout anode by the avalanche electrons and ions motion in the amplification gap. The total signal induced by the avalanche ions and the electrons, which are generated by 5.9 keV photon can be calculated by Garfield, as shown in Fig. 6. The separate time of different peaks is near 1 ns, which is due to the distance between the nearby electron clusters in the drift gap. The leading-edge of the pulse is near 25 ns, which is determined by the space distribution and the diffusion of primary electron clusters in the drift gap. The recovery part is due to the movement of the ions and the rise time is near 300 ns.

4 Conclusion

In summary, a full 3D simulation of Micromegas

is performed to study the performance of the Micromegas detector. The simulation results are nearly consistent with the experimental data, including the ratio of total energy peak to escape peak of X-ray in argon, and the change of electron collection efficiency with electric field ratio $E_{\text{amp}}/E_{\text{drift}}$. The percents of argon ions participating in the penning effect are analyzed in different gas mixtures. The energy resolutions do not change with the voltage of mesh in different gas mixtures. The results of the simulations provide important information on the Micromegas design, making and operation.

We thank Dr. Rob Veenhof, Dr. Ming Shao and Yi Zhou for their help on this work and thank Professor Tianchi Zhao and Professor Zhengguo Zhao for their fruitful discussions.

References

- 1 Giomataris Y et al. Nucl. Instrum. Methods A, 1996, **376**: 29
- 2 Maxwell 3D Field Simulator. Available: <http://wwwinfo.cern.ch/ce/ae/Maxwell/Maxwell.html>
- 3 Veenhof R, Garfield. Available: <http://consult.cern.ch/writeup/garfield>
- 4 TANG Hao-Hui et al. Chinese Physics C, 2008, 0254
- 5 ORTEC 142AH Preamplifier Available: <http://www.ortec-online.com/electronics/preamp/142ah.htm>
- 6 Biagi S, Magboltz. Available: <http://consult.cern.ch/writeup/magboltz>
- 7 Smirnov I, HEED. Available: <http://consult.cern.ch/writeup/heed>
- 8 Colas P et al. Nucl. Instrum. Methods A, 2004, **535**: 226
- 9 Veenhof R. Nucl. Instrum. Methods A, 2006, **563**: 291
- 10 Ramo S. Proc. IRE, 1939, **27**: 584–585